



Response of silicon solar cells to neutrons in post-detonation monitoring

Praneeth Kndlakunta^{a,*}, Matthew Van Zile^b, Susan White^b, Lei Raymond Cao^{a,b}

^a Nuclear Engineering Program, Department of Mechanical and Aerospace Engineering, The Ohio State University, Columbus, OH, USA

^b Nuclear Reactor Laboratory, College of Engineering, The Ohio State University, Columbus, OH, USA



A B S T R A C T

In this study, we evaluated the feasibility of using solar photovoltaic (PV) panels for the detection of prompt neutrons from a nuclear detonation. Monte Carlo (MC) simulations were performed to evaluate the response of silicon (Si) solar cells (SCs) to neutrons and support the experiments. The response of Si SCs to fission spectrum neutrons was measured experimentally using the fast neutron beam of a research reactor. Steady-state neutron measurements indicated a clear response of the Si SCs, which correlated with changes in the neutron intensity. Time-modulated neutron measurements performed using a neutron chopper demonstrated a clear transient response of Si SCs to neutrons, which was observed in the signal power spectral density plots containing peaks corresponding to frequencies of neutron pulses produced by the chopper. The resulting signal was found to be small, which was attributed to the extremely small active neutron interaction volume inside the SCs. In a real detonation scenario, the transient neutron flux is expected to be higher, and the effective neutron interaction volume of large area solar PV panels is much larger, which could significantly boost the signal. The study, overall, demonstrated the potential of large area solar PV panels or a solar farm for prompt detection and identification of a nuclear detonation.

1. Introduction

Nuclear detonations result in the emission of intense electromagnetic radiation that covers a wide range of wavelengths corresponding to gamma-rays, X-rays, intense light, and radiowaves. There are neutrons emitted during the nuclear fission reactions (prompt neutrons) and neutrons from decay process of a few fission products (delayed neutrons). A significant amount of energy is released in the form of air blast/shock wave and comprises seismic waves, air pressure waves, and infrasound [1]. The interaction of such an intense energy source with the environment can overwhelm a single sensor or a monitoring network. The manmade infrastructure present in urban environments, including solar photovoltaic (PV) panels, can function as sensors for detecting the immense radiation energy emitted during a nuclear detonation. PV panels offer a means to measure high-energy radiation, such as neutrons, gamma-rays, and X-rays, generated by the detonation. By detecting the sudden and abnormal changes in the baseline signal of the PV panels, it becomes possible to promptly identify a nuclear detonation. Additionally, analyzing the persistent and measurable signatures left in the PV devices due to radiation interactions during the detonation can provide valuable post-detonation forensics information.

The inherent sensitivity of a PV material such as silicon (Si) to gamma-rays (e.g., through photoelectric, Compton, and pair-production interactions) and neutrons (e.g., neutron scattering and energy threshold reactions), and the active p-n junction inside a solar cell (SC) make the

PV device responsive to the nuclear radiation emitted in a nuclear explosion. The sheer amount of radiation energy from a nuclear blast might offset the low efficiency of a Si-based SC to high-energy gammarays and neutrons, resulting in a detectable signal. Moreover, the interaction of thermalized neutrons with the p-type dopant boron in Si may enhance the overall sensitivity of a Si SC to the neutron spectrum of nuclear detonation. In addition, neutron scattering/absorption by assembly materials within the SC may also provide measurable data capable of predicting the weapon yield. The prompt radiation from a nuclear detonation is an intense but short pulse of gamma rays and neutrons that are emitted in a few microseconds, followed by an intense optical radiation pulse that lasts much longer. The high intensity prompt pulse of gamma-rays and neutrons may produce a measurable transient signal in solar PV devices due to their high transient flux before the arrival of the optical pulse.

The total number of neutrons released in the detonation of a well-designed weapon is, roughly, 10^{23} neutrons per kT of fission yield [2], with an average energy of 2 MeV. Assuming no attenuation, 2 MeV neutron fluence at an object located at 1 km distance (r) from the detonation point, is $- \text{fluence at detonation center}/4\pi r^2$. This gives a neutron fluence of $\sim 8 \times 10^{11} \text{ cm}^{-2}$ per kT. Due to variations in interaction mechanisms, attenuation characteristics, and speeds between neutrons and gamma-rays, the arrival of the prompt neutron pulse at the solar panel location will occur after the prompt gamma-ray pulse. The resulting prompt signal output of SCs in response to neutrons is expected

* Corresponding author.

E-mail address: kndlakunta.1@osu.edu (P. Kndlakunta).

to be different from that of gamma-rays in terms of the amplitude, onset time and temporal characteristics. For post-detonation nuclear forensics analysis, it is important to understand neutron induced signal change in SCs in addition to that of gammas and separate it from the response to gamma-rays.

There is a large amount of literature [3–17] on SCs' radiation damage study due to their application in space where gamma-rays and protons constitute the major radiation. However, there have been very limited studies on the radiation monitoring applications of solar PV devices. An early study evaluated Si SCs for X-ray and gamma-ray dosimetry and radiation monitoring [18]. A solar panel was demonstrated as a large area radiation detector with directional sensitivity for monitoring direct and scattered X-rays, and gamma-rays [19]. Commercial monocrystalline Si SCs as well as low power amorphous Si cells were also evaluated as gamma-ray dosimeters [20,21]. A more recent study evaluated gamma radiation monitoring and radiation effects in solar PV devices using experiments, simulations, and analytical calculations [22].

Although there has been some research on X-ray and gamma-ray dosimetry using SCs, neutron monitoring applications of solar PV devices have been rarely reported. In particular, *in situ* studies that focused on the change in baseline current of SCs upon sudden infusion of large amount of radiation energy of MeV neutrons have been very limited. In the current study, we evaluated the feasibility of using solar PV panels as the sensors of the characteristic prompt neutron signature of a nuclear detonation. We performed Monte Carlo (MC) simulations to understand the interaction of fast neutrons with Si SCs. We also evaluated the steady-state and transient response of SCs to neutrons using commercial-off-the-shelf (COTS) Si SC modules and the fast neutron beam facility at The Ohio State University Research Reactor (OSURR).

2. Solar cells interaction with neutrons

The neutron induced nuclear reactions in Si provide insight into the interaction mechanism of the Si SC with neutrons. Nuclear reactions that are relevant to the discussions in this paper are summarized in Table 1 which also lists their neutron cross section, neutron energy threshold and the Q-value.

We performed Monte Carlo (MC) simulations to further understand the response of a Si SC to fast neutrons and support the experimental study. Therefore, the interaction of fast neutrons with Si and other SC materials was simulated using MC models built in Geant4 [24]. A simplified model of a poly-crystalline Si (poly-Si) SC including all the material layers (see Fig. 1a) was created in Geant4. A mono-energetic neutron source was created, which emitted a neutron beam orthogonal to the front epoxy surface of the SC (Fig. 1b). Simulations were performed for different incident neutron energies. The total energy deposited within the Si layer of the SC was calculated, considering the energy deposited by all the energy loss processes, while accounting for the transport of secondary particles through different SC material layers.

Fig. 2 shows the total dose deposited by neutrons in the Si layer of a

Table 1
Neutron-induced reactions in a Si solar cell [23].

Nuclear reaction	Q-Value (MeV)	Threshold Energy (MeV)	Neutron cross-section (b)		
			14 MeV	2 MeV	0.025 eV
$^{28}\text{Si}(n,n')$ ^{28}Si	0	0	0.662	2.648	1.991
$^{28}\text{Si}(n,n')$ ^{28}Si (first excited state)	-1.779	1.843	0.124	0.099	-
$^{28}\text{Si}(n,\alpha)$ ^{25}Mg	-2.654	2.746	0.178	-	-
$^{28}\text{Si}(n,\gamma)$ ^{28}Al	-3.860	4.004	0.279	-	-
$^{30}\text{Si}(n,\gamma)$ ^{31}Si	-6.592	0	0.001	0.001	0.107
$^{31}\text{Si} \rightarrow ^{31}\text{P}$					
$^{10}\text{B}(n,\alpha)$ ^7Li	2.8	0	0.500	0.050	3842

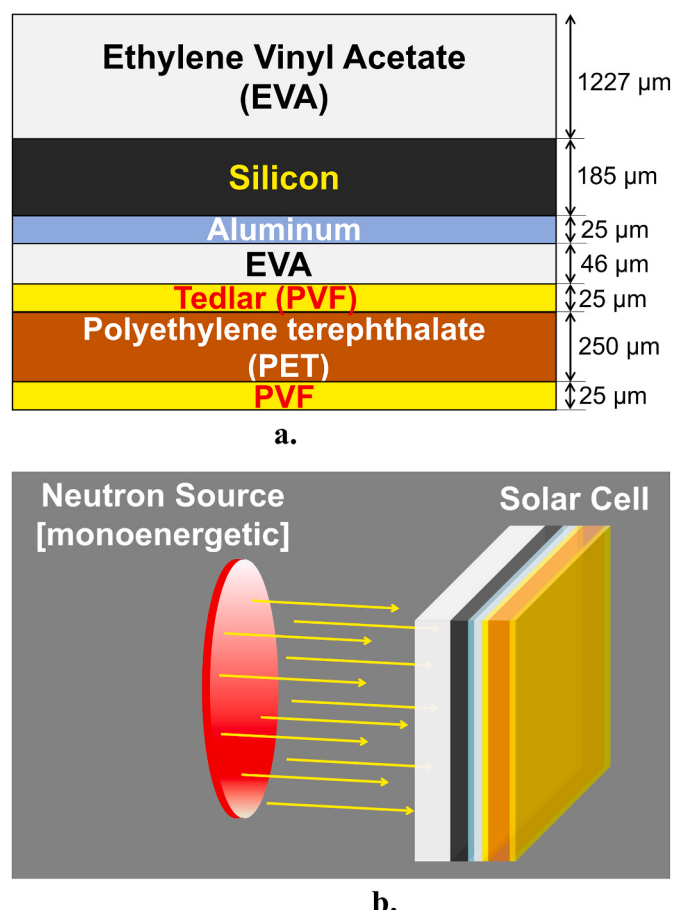


Fig. 1. a. Schematic of the poly-Si solar cell (SC) structure used in the MC simulations showing different material layers. b. Visualization of a neutron beam illuminating the solar cell in the Geant4 MC model.

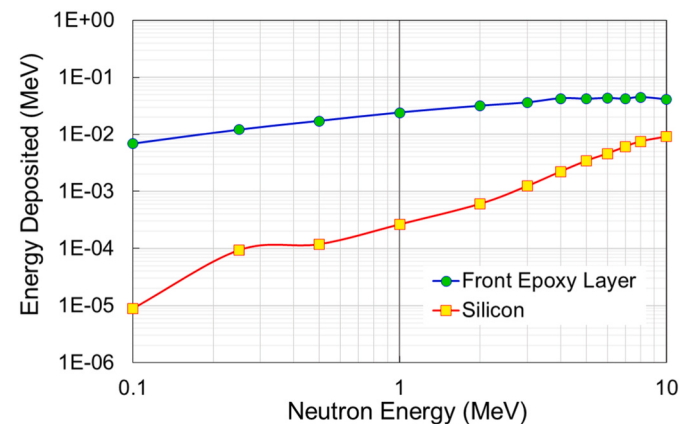


Fig. 2. Monte Carlo (MC) simulation result of neutron dose deposited in the Si layer and the front epoxy layer of the poly-Si SC as a function of incident neutron energy.

poly-Si SC as a function of the incident neutron energy. The neutron dose in Si continues to increase with the increase in incident neutron energy with an indication that the neutron dose reaches saturation at higher energies (>10 MeV). The sensitivity of the poly-Si SC to neutrons might be enhanced due to the presence of other organic and hydrogenous polymer layers in its structure. To understand this effect, the dose in the front epoxy layer was also calculated as a function of neutron energy, which is much higher than that in Si layer (Fig. 2). As in the case of Si,

neutron dose in epoxy increases with increase in the energy but is seen to saturate faster at ≥ 4 MeV.

3. Experiments

The SC neutron measurements were performed at the fast neutron beam facility of the OSURR, which delivers a reactor-spectrum neutron beam with 1.25-inch (32 mm) diameter. The total neutron flux at the exit of the fast neutron beam collimator at full reactor power ($450 \text{ kW}_{\text{th}}$) is $2.3 \times 10^7 \text{ cm}^{-2} \text{ s}^{-1}$, with a thermal neutron component (neutron energy, $E_n < 0.5 \text{ eV}$) of $8.0 \times 10^6 \text{ cm}^{-2} \text{ s}^{-1}$ and an epithermal (epi)-cadmium (Cd) flux ($E_n > 0.5 \text{ eV}$) of $1.5 \times 10^7 \text{ cm}^{-2} \text{ s}^{-1}$. The OSURR beam port that delivers the fast neutron beam contains a 4-inch-thick bismuth block near the reactor core that filters the gamma-rays from the core. The beamline has a gamma-ray shutter inside the reactor shielding wall, which consists of a drum filled with 1/16-inch lead shot, that, when closed, offers about 8-inches of gamma shielding significantly attenuating the residual gamma-rays and gamma-rays from other extraneous sources in the beam. The gamma shutter was also found to attenuate the neutron flux significantly. In this case, the total neutron flux at the beam collimator exit with the shutter closed at $450 \text{ kW}_{\text{th}}$ is $2.9 \times 10^5 \text{ cm}^{-2} \text{ s}^{-1}$, with a thermal neutron component of $3.0 \times 10^4 \text{ cm}^{-2} \text{ s}^{-1}$, and an epi-Cd flux of $2.6 \times 10^5 \text{ cm}^{-2} \text{ s}^{-1}$. During the measurements, the gamma shutter was closed and opened intermittently to compare the SCs response to neutrons in both cases.

3.1. Design

We created another MC model in Geant4 to support and guide our experimental design for evaluating SC response to neutrons using OSURR fast neutron beam. To maximize the neutron signal output from the SC and ensure that it is measurable experimentally, we simulated an array of SCs while taking into account the constraints for experimental setup at the fast beam facility. Thus, the previous MC model was extended from a single poly-Si SC to a linear poly-Si SC array. As in the previous model, a disc neutron source was created, which emitted a neutron beam orthogonal to the SC surface (Fig. 3a). The energy distribution of neutrons matched that of the neutron spectrum at the exit of the fast neutron beam collimator (Fig. 3b). The total energy deposited within the Si layer of each SC in the array was calculated from simulating 10 million neutron histories. Different orientations of the SC array with respect to the beam direction were examined, and the spacing between adjacent SCs in the array was also tuned to ultimately determine a configuration that was both practical and yielded the highest possible sum of energies deposited in the Si layer of individual SCs.

A representative result from the MC simulations shown in Fig. 4a indicates the energy deposition of neutrons (see Fig. 3b) in 20 individual SCs stacked together. In this case, the spacing between the adjacent SCs was 5 mm and the SC array was aligned orthogonal to the beam direction, which was found to be an optimal configuration for the experiments. As expected, the energy deposited is the highest for the first SC facing the beam and decreases steadily for successive SCs. The total energy deposited from the interaction of neutrons with the SC array i.e., the sum of energy depositions in all individual SCs, was calculated and converted into an equivalent short-circuit electric current (I_{sc}) based on the total neutron flux and the beam size. The simulations indicated a total I_{sc} of $\sim 65 \text{ nA}$ from 20 SCs in response to the neutrons (Fig. 4b). By introducing additional SCs beyond the 20 in the array, the gain in I_{sc} was estimated to be very low and practically insignificant. It must, however, be noted that the I_{sc} calculation in the simulations assumed 100% charge collection efficiency of the charge deposited in the Si layer of the SCs. In reality, the charge collection would be lesser, as the SC depletion region is extremely thin ($< 1 \mu\text{m}$), and thus, the charge generated at distances greater than a diffusion length from the depletion region is not collected.

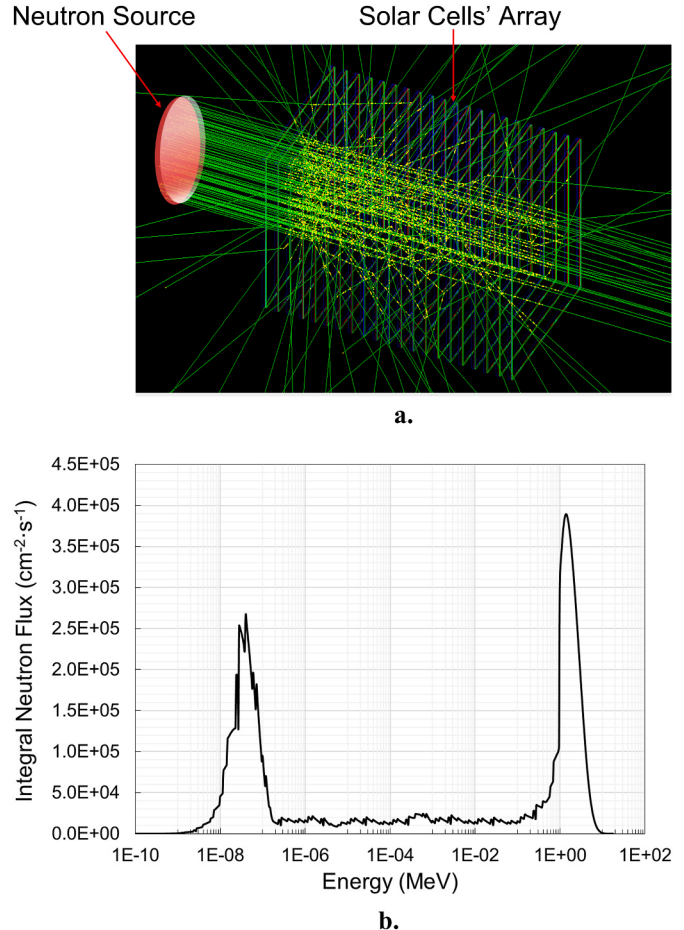


Fig. 3. a. Visualization of a neutron beam illuminating a linear array of poly-Si solar cells (SCs) in the Geant4 MC model. b. Energy spectrum of neutrons at the exit of the fast neutron beam collimator at OSURR.

3.2. Steady-state neutron measurements

Based on the simulation results, we assembled a linear array of 21 poly-Si SC modules connected electrically in parallel (see Fig. 5a). This configuration enabled the measurement of the net I_{sc} i.e., the sum of I_{sc} of all individual SC modules in response to neutrons. The SC module array (SCMA) was placed at the exit of the OSURR fast beam collimator (Fig. 5a) and exposed to the neutron flux at full reactor power. The total area of PV exposed to neutrons is 8 cm^2 . A schematic of the steady-state neutron measurement setup is shown in Fig. 5b. In these measurements, the total I_{sc} of the SCMA was measured using an electrometer (Keithley 6514) and the data was continuously acquired using a LabVIEW program on the PC.

The steady-state I_{sc} response of SCMA to fast neutrons from a thermal fission spectrum is shown in Fig. 6. Results indicate a clear response of the SCMA that correlates with the changes in neutron intensity as the internal gamma shutter was closed (i.e., gamma-rays removed by filter) and opened (i.e., without gamma-filter). When the gamma shutter was closed, the response was lower, which is most possibly due to the attenuation of a significant portion of the neutron flux, along with that of gamma-rays. Although the gamma-ray content in the beam is expected to be low, the individual contributions of neutrons and gamma-rays to the SCMA response could not be quantitatively determined based on these results. In addition, the steady-state measurements indicate a very low I_{sc} of the SCMA, which is attributed to the extremely small active volume of the SCs for neutron interaction (e.g., small beam area, extremely low active thickness of SCs).

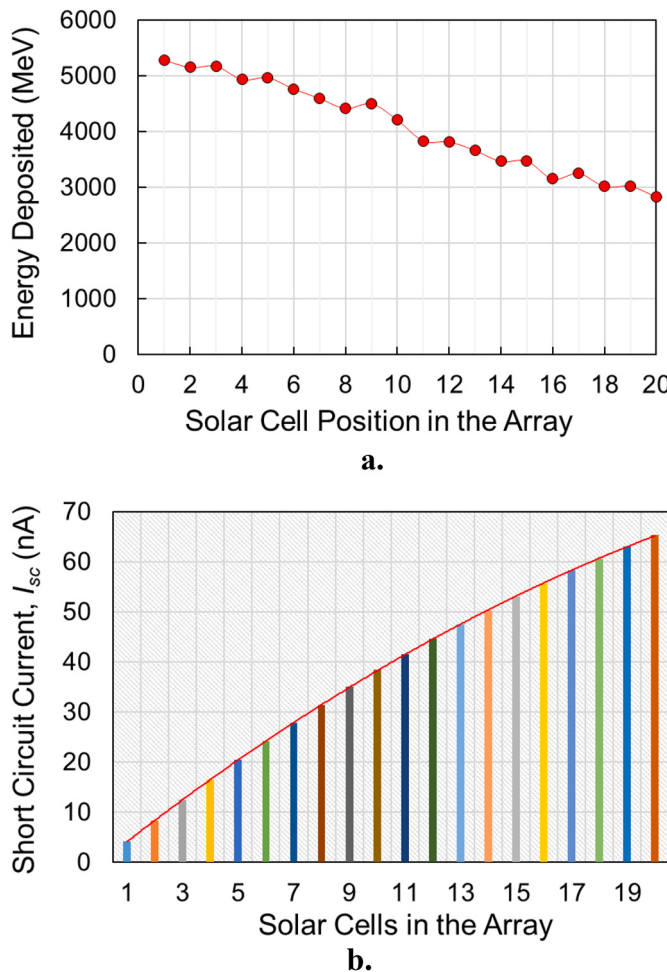


Fig. 4. **a.** Energy deposited in the Si layer of individual solar cells (SCs) in the array calculated from Monte Carlo (MC) simulation of 10 million neutron histories. The energy spectrum of source neutrons matched that of the neutron beam at the collimator exit at OSURR. **b.** The equivalent total short-circuit current (I_{sc}) predicted from the SCs connected in parallel in the array.

3.3. Transient neutron measurements

The fast neutron beam at OSURR is also equipped with an external neutron beam chopper that produces a time-modulated neutron beam with pulsed neutrons. The SCMA transient response measurements were performed using the neutron beam chopper which is a 12-inch diameter cylinder made of borated HDPE, placed at the exit of the beam collimator with its axis of rotation perpendicular to the beamline (Fig. 7a). The borated HDPE cylinder has a rectangular aperture on its lateral surface of length equal to the cylinder diameter. The aperture is always perpendicular to the cylinder axis, and when aligned with the collimator exit, provides the maximum neutron intensity through the chopper. The neutron pulses exiting the chopper have a frequency twice that of the chopper rotational frequency, with a slow rise to the maximum and an equally slow fall to the minimum. The rise time, fall time, and the pulse period are all determined by the chopper rotational frequency, whereas the pulse duty cycle is fixed as it depends only on the aperture height and the cylinder circumference.

The chopper was operated at different rotational frequencies during the SCMA transient response measurements. The I_{sc} transient signal from the SCMA was connected to the input of a transimpedance amplifier (Thorlabs AMP100, 1 kHz Bandwidth) set to a gain of 10 MV/A (Fig. 7b). The transient voltage signal from the amplifier was measured and acquired using an oscilloscope (Keysight MSO-X 3034T) for subsequent

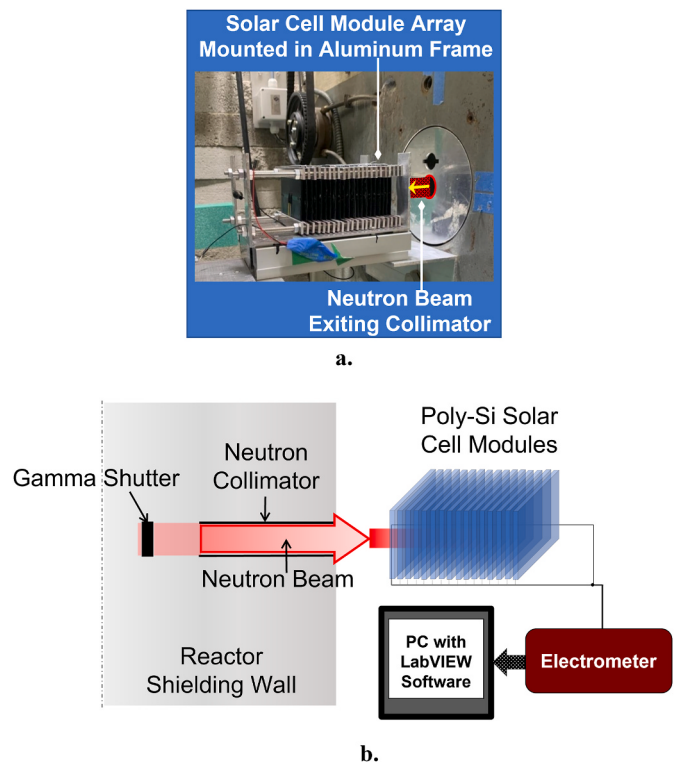


Fig. 5. **a.** Picture showing the arrangement of the solar cell module array (SCMA) mounted in an aluminum frame and placed at the exit of the OSURR fast beam collimator, total 8 cm² of PV are exposed to the neutron beam of 32 mm in diameter. **b.** Schematic of the experimental setup used at OSURR fast neutron beam facility for measuring the steady-state response of Si solar cells (SCs) to neutrons.

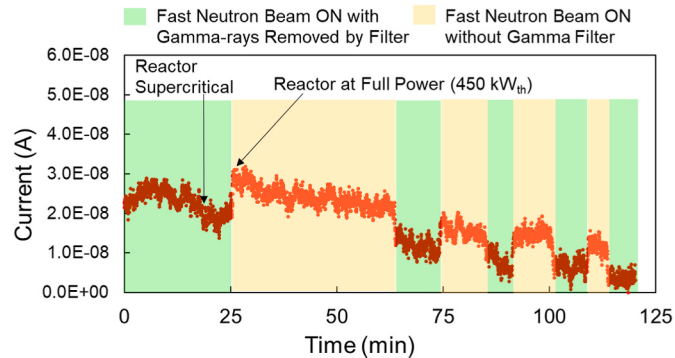


Fig. 6. Steady-state short-circuit current (I_{sc}) response of the solar cell module array (SCMA) to the fast neutron beam of the OSURR resulting from a thermal fission spectrum at 450 kW_{th} reactor power.

data analysis and interpretation.

Fig. 8 shows the transient response of the SCMA under different measurement conditions at 5 Hz chopper frequency. The corresponding voltage waveforms recorded when a) fast neutron beam was ON without any gamma filter (i.e., gamma shutter was open, at full reactor power), b) fast neutron beam was ON with gamma-rays removed by filter (i.e., gamma shutter was closed, at full reactor power, and c) fast neutron beam was OFF without any gamma filter (i.e., gamma shutter was open, post reactor shut down) overlap with each other and thus, the SCMA response to neutrons is not easily distinguishable. Results in the time domain have not clearly indicated the response to neutrons. Background measurements conducted prior to turning on the reactor indicated that the output voltage of the SCMA was approximately 600 mV at a

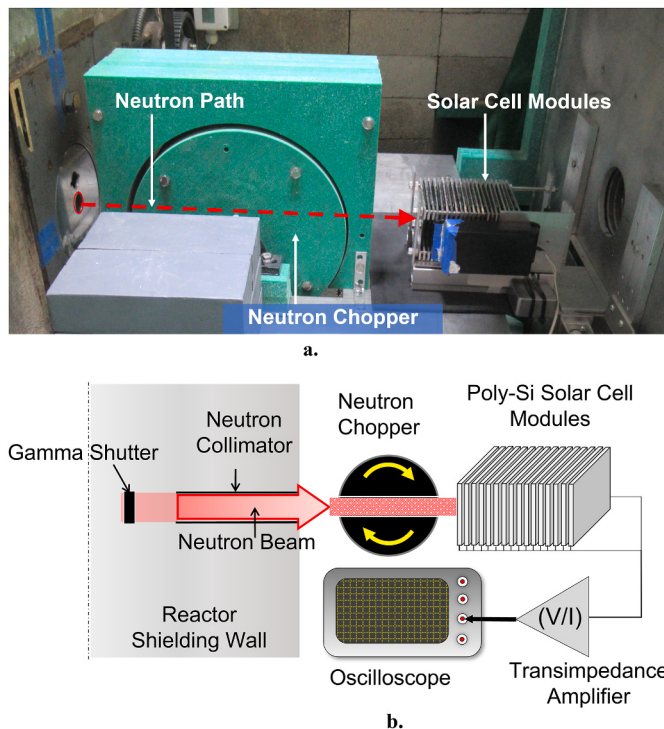


Fig. 7. a. Picture showing the arrangement of the solar cell module array (SCMA) and the fast neutron mechanical chopper with respect to the beam collimator exit. b. Schematic of the experimental setup used at OSURR fast neutron beam facility for measuring the transient response of solar cells (SCs) to neutrons.

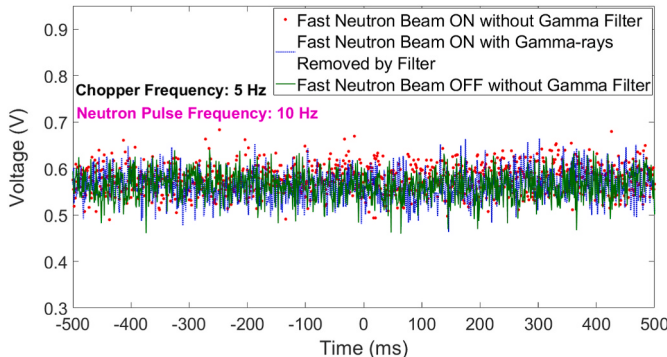


Fig. 8. Time domain results of the SCMA transient response to neutrons at 5 Hz chopper rotational frequency. Waveforms of the amplifier output voltage signal are shown under different measurement conditions.

transimpedance gain of 10 MV/A. This value corresponds to an I_{sc} of around 60 nA. The observed I_{sc} can be attributed to ambient light leakage into the setup due to suboptimal light shielding around the SCMA. In contrast, the signal induced by neutrons is anticipated to be significantly weaker, and thus, it was not clearly distinguishable in the results presented in Fig. 8. However, it is important to note that in an actual nuclear detonation scenario, the transient neutron flux is much higher, and the effective neutron interaction volume provided by large-area solar PV panels or solar farms is substantially larger. Consequently, this increased interaction volume has the potential to produce a measurable output signal.

For better interpreting the results, we acquired the waveform data in the frequency domain (*i.e.*, as FFT of the voltage signal) under different conditions as listed before. Fig. 9 shows the plots of power spectral density (PSD) of the amplifier's output signal at different chopper

rotational frequencies. In the case of 10 Hz chopper frequency (Fig. 9a), for example, when the gamma shutter was open at full reactor power, a peak was observed at 20 Hz, which is the frequency of the neutron pulses at 10 Hz chopper frequency. When the gamma shutter was closed at full reactor power, the 20 Hz peak was not found in the PSD, which could be due to the significant attenuation of neutrons. Data collected immediately after the reactor was shut down, and with the shutter open also showed no 20 Hz peak in the PSD, which indicates that the contribution of delayed gamma-rays from fission product decay to the SCMA response is negligible. However, the 10 Hz frequency peak is present in all three cases, which is attributed to the microphonic noise induced from the chopper rotation. Based on these observations, the peak at 20 Hz could be resulting from neutrons. We obtained similar results at other chopper frequencies (Fig. 9b-d). For example, at 5 Hz chopper rotational frequency, when the gamma shutter was open at full reactor power, a peak was observed at 10 Hz in the PSD plot (Fig. 9b), which is the neutron pulse frequency corresponding to 5 Hz chopper rotation. These results indicated that the Si SCs used in this study showed response to the fast neutrons.

Our experiments and MC simulations demonstrate the feasibility to detect and identify a nuclear detonation using solar PV panels by measuring the prompt neutron radiation released in the explosion. While the results presented here showed the SCs response to fission spectrum neutrons from a reactor, the energy distribution of neutrons emitted in a nuclear explosion and that at the location of a solar farm, both, may be very different from that used in our study.

4. Delayed effects in solar cells from neutron irradiation

We also investigated delayed radiation effects in SCs for their use in post-detonation nuclear forensics. COTS Si SCs were irradiated by neutrons to study the delayed radiation effects in SCs due to neutron activations. Irradiations were performed at the pneumatic irradiation facility (Rabbit Facility) of the OSURR, which provided a total integral neutron flux of $\sim 3.4 \times 10^{12} \text{ cm}^{-2} \text{ s}^{-1}$. The cells were irradiated to a neutron fluence equivalent to that from detonation of a 500 kT fission-based weapon at 1000 yards from the detonation point. This fluence was determined to be $\sim 4.8 \times 10^{14} \text{ cm}^{-2}$ based on the data from literature [1, 2]. Two sets of SCs, each comprising one poly-Si cell (AMX Solar, SP-53X30-1-DK) and one mono-Si cell (ANY SOLAR, KXOB25-12 × 1F) were irradiated. One set of poly-Si and mono-Si cells were covered by cadmium (Cd) sheet, whereas the other set was uncovered (bare). This was done to block thermal neutrons using Cd, thereby isolating the fast neutron effects, if any, in the SCs.

All irradiated SCs were counted by gamma-ray spectroscopy using HPGe detector at the OSU nuclear reactor lab. However, the cells were left to decay for 9 days before the counting owing to radiation safety and other facility constraints. The gamma-ray spectra resulting from neutron activation of the irradiated SCs are shown in Fig. 10. The gamma spectra primarily indicate energy peaks corresponding to silver, antimony, and tin in case of poly-Si devices (Fig. 10a); and peaks corresponding to bromine and gold in case of mono-Si devices (Fig. 10b). It is possible that all the short-lived radionuclides have decayed out to a very low activity. After 9 days of decay followed by gamma counting, the SCs were measured for their current-voltage ($I-V$) characteristics under dark. There was no indication of a possible I_{sc} induced by the residual radioactivity from neutron activation.

The feasibility of post-detonation forensics was demonstrated by measuring the long-lived radionuclide gamma-rays resulting from neutron activation of Si SCs at a research reactor.

5. Conclusion

In summary, steady-state response of Si solar cells (SCs) to neutrons was measured and shown to correlate with changes in neutron intensity. A clear transient response of Si SCs to neutrons was demonstrated by the

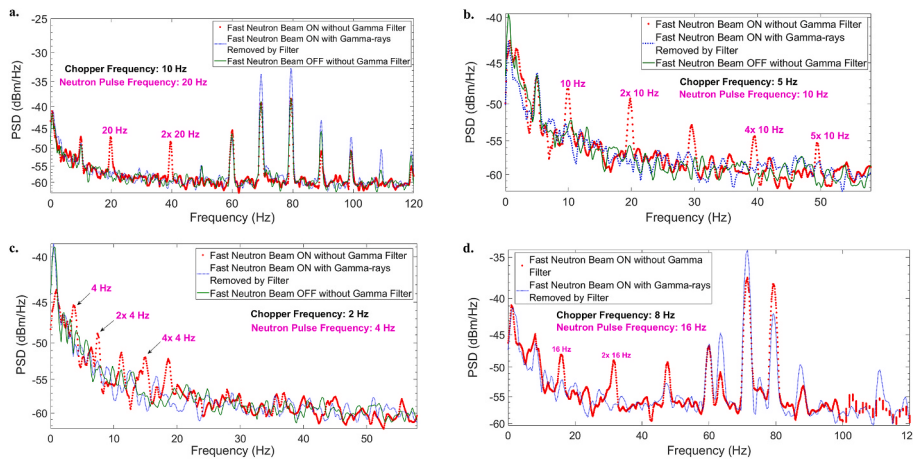


Fig. 9. Frequency domain results of the SCMA transient response at different chopper rotational frequencies **a.** 10 Hz **b.** 5 Hz **c.** 2 Hz **d.** 8 Hz. Shown are the power spectral density (PSD) plots of the amplifier output voltage signal acquired under different measurement conditions.

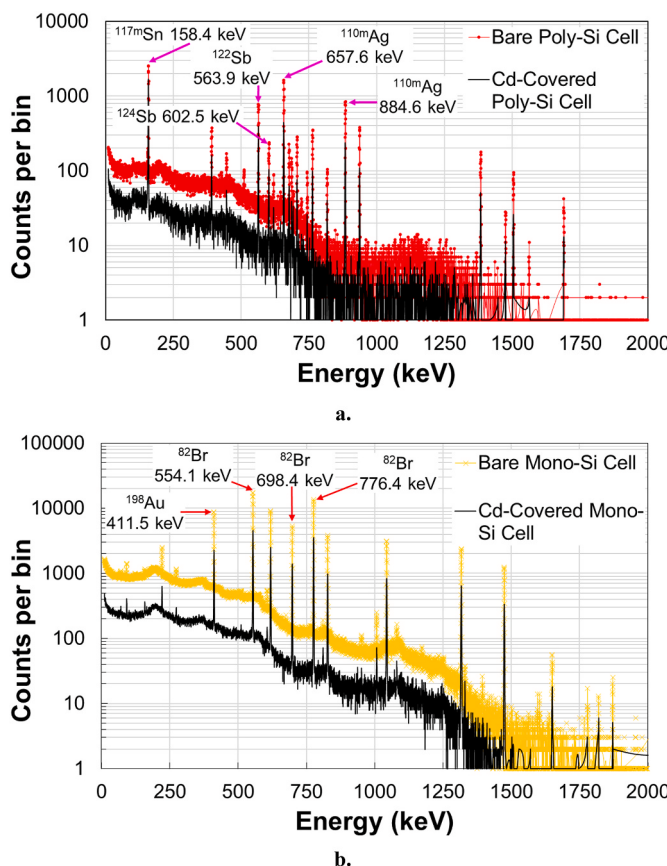


Fig. 10. Gamma-ray spectra of irradiated Si SCs: **a.** Cd-covered and bare poly-Si cells **b.** Cd-covered and bare mono-Si cells.

time-modulated neutron measurements using neutron chopper. While the resulting neutron signal from the SCs was small, the total irradiated SC area was only 8 cm^2 . In contrast, a roof top SC coverage is about 200 square feet ($185,806 \text{ cm}^2$) for a small home and 1000 square feet ($929,030 \text{ cm}^2$) for a larger home, which could significantly boost the signal from neutron interaction and yield high signal-to-noise ratio. Our study demonstrated the potential of large area solar PV panels or a solar farm for prompt detection and identification of a nuclear detonation.

We suggest that future research should be directed towards expanding SC areal coverage as much as possible given the experimental

conditions. This expansion should be supported by a comprehensive simulation of the radiation field; and the use of fast switching sources could improve the verification of the PV panel transient response. Additionally, several further steps can be taken to advance this technology to a mature stage. These include data reduction to establish a prompt signature library, creating a roadmap outlining the abilities of other infrastructure components' responses (e.g., roof top Si solar panels) to post-detonation signatures, and integrating solar charge controllers and software.

Declaration of competing interest

The authors declare that they have no known competing financial interests or personal relationships that could have appeared to influence the work reported in this paper.

Acknowledgments

We would like to acknowledge the support of OSU Nuclear Reactor Laboratory and the assistance of the reactor staff members for the irradiation services provided. We are also grateful to Dr. John McClory at Airforce Institute of Technology, Dr. Jinsong Huang at University of North Carolina at Chapel Hill, and Dr. Jeremy Osborn and Dr. Richard Harrison at Sandia National Laboratories for the helpful discussions. This research has been performed with the financial support from the U. S. Department of Defense, Defense Threat Reduction Agency under Grant HDTRA-11910024.

References

- [1] S. Glasstone, P.J. Dolan, *The Effects of Nuclear Weapons*, US Department of Defense, 1977.
- [2] K. Kramer, T. Dant, A. Li, K. Millage, Publicly Released Prompt Radiation Spectra Suitable for Nuclear Detonation Simulations, Revision 1, Applied Research Associates Inc Arlington Va Arlington United States, 2017.
- [3] M. Yamaguchi, S.J. Taylor, M.-J. Yang, S. Matsuda, O. Kawasaki, T. Hisamatsu, Analysis of radiation damage to Si solar cells under high-fluence electron irradiation, *Jpn. J. Appl. Phys.* 35 (1996) 3918–3922, <https://doi.org/10.1143/jjap.35.3918>.
- [4] D. Nikolić, K. Stanković, L. Timotijević, Z. Rajović, M. Vujisić, Comparative study of gamma radiation effects on solar cells, photodiodes, and phototransistors, *Int. J. Photoenergy* 2013 (2013) 843174, <https://doi.org/10.1155/2013/843174>.
- [5] B. Simić, D. Nikolić, K. Stanković, L. Timotijević, S. Stanković, Damage induced by neutron radiation on output characteristics of solar cells, photodiodes, and phototransistors, *Int. J. Photoenergy* 2013 (2013).
- [6] W. Luft, Effects of electron irradiation on N on P silicon solar cells, *Adv. Energy Convers.* 5 (1965) 21–41, [https://doi.org/10.1016/0365-1789\(65\)90011-1](https://doi.org/10.1016/0365-1789(65)90011-1).
- [7] J. Mandelkorn, L. Schwartz, J. Broder, H. Kautz, R. Ulman, Effects of impurities on radiation damage of silicon solar cells, *J. Appl. Phys.* 35 (1964) 2258–2260.

- [8] W. Rosenzweig, F.M. Smits, W.L. Brown, Energy dependence of proton irradiation damage in silicon, *J. Appl. Phys.* 35 (2004) 2707–2711, <https://doi.org/10.1063/1.1713827>.
- [9] M. Alurralde, M.J.L. Tamasi, C.J. Bruno, M.G.M. Bogado, J. Plá, J.F. Vázquez, J. Durán, J. Schuff, A.A. Burlon, P. Stolar, Experimental and theoretical radiation damage studies on crystalline silicon solar cells, *Sol. Energy Mater. Sol. Cells* 82 (2004) 531–542.
- [10] D.M. Tobnaghi, A. Rahnamaei, M. Vajdi, Experimental study of gamma radiation effects on the electrical characteristics of silicon solar cells, *Int. J. Electrochem. Sci.* 9 (2014) 2824–2831.
- [11] M. Yamaguchi, S.J. Taylor, M. Yang, S. Matsuda, O. Kawasaki, T. Hisamatsu, High-energy and high-fluence proton irradiation effects in silicon solar cells, *J. Appl. Phys.* 80 (1996) 4916–4920.
- [12] N. Horiuchi, T. Nozaki, A. Chiba, Improvement in electrical performance of radiation-damaged silicon solar cells by annealing, *Nucl. Instruments Methods Phys. Res. Sect. A Accel. Spectrometers, Detect. Assoc. Equip.* 443 (2000) 186–193.
- [13] F.A. Junga, G.M. Enslow, Radiation effects in silicon solar cells, *IEEE Trans. Nucl. Sci.* 6 (1959) 49–53.
- [14] J.R. Srour, J.W. Palko, D.H. Lo, S.H. Liu, R.L. Mueller, J.C. Nocerino, Radiation effects and annealing studies on amorphous silicon solar cells, *IEEE Trans. Nucl. Sci.* 56 (2009) 3300–3306, <https://doi.org/10.1109/TNS.2009.2034329>.
- [15] D.J. Curtin, R.L. Statler, Review of radiation damage to silicon solar cells, *IEEE Trans. Aero. Electron. Syst.* (1975) 499–513.
- [16] W. Rosenzweig, Space radiation effects in silicon devices, *IEEE Trans. Nucl. Sci.* 12 (1965) 18–29, <https://doi.org/10.1109/TNS.1965.4323897>.
- [17] H.H. Sander, B.L. Gregory, Transient annealing in semiconductor devices following pulsed neutron irradiation, *IEEE Trans. Nucl. Sci.* 13 (1966) 53–62, <https://doi.org/10.1109/TNS.1996.4324346>.
- [18] K. Scharf, Photovoltaic effect produced in silicon solar cells by x-rays and gamma rays, *J. Res. Natl. Bur. Stand. Sect. A Phys. Chem.* (1960), <https://doi.org/10.6028/jres.064a.029>.
- [19] S. Abdul-Majid, Use of a solar panel as a directionally sensitive large-area radiation monitor for direct and scattered x-rays and gamma-rays, *Int. J. Radiat. Appl. Instrum. Appl. Radiat. Isot.* 38 (1987) 1057–1060, [https://doi.org/10.1016/0883-2889\(87\)90070-0](https://doi.org/10.1016/0883-2889(87)90070-0).
- [20] H.M. Diab, A. Ibrahim, R. El-Mallawany, Silicon solar cells as a gamma ray dosimeter, *Measurement* 46 (2013) 3635–3639.
- [21] V. Fugaru, R.O. Dumitrescu, C.D. Negut, Low-power photovoltaic cells batteries used as gamma radiation dose estimators, *Rom. J. Phys.* 63 (2018) 903.
- [22] P. Kandlakunta, M. Van Zile, L.R. Cao, Silicon solar cells for post-detonation monitoring and gamma-radiation effects, *Nucl. Sci. Eng.* 196 (2022) 1383–1396, <https://doi.org/10.1080/00295639.2022.2091905>.
- [23] Brookhaven National Laboratory, Evaluated nuclear data file (ENDF), *Natl. Nucl. Data Cent.* (2018). <https://www.nndc.bnl.gov/endf/>. March 25, 2023.
- [24] S. Agostinelli, J. Allison, K. al Amako, J. Apostolakis, H. Araujo, P. Arce, M. Asai, D. Axen, S. Banerjee, G. Barrand, GEANT4—a simulation toolkit, *Nucl. Instruments Methods Phys. Res. Sect. A Accel. Spectrometers, Detect. Assoc. Equip.* 506 (2003) 250–303.